Reactive inkjet printing of calcium alginate hydrogel porogens—a new strategy to open-pore structured matrices with controlled geometry†

Joseph T. Delaney, Jr.,[abc] Albert R. Liberski,[bc] Jolke Perelaer[bc] and Ulrich S. Schubert*[abc]

Received 3rd November 2009, Accepted 14th December 2009
First published as an Advance Article on the web 6th January 2010
DOI: 10.1039/b922888h

Taking advantage of inkjet's ability to dispense uniform droplets in the picolitre/nanolitre ranges of volumes, we have generated reversible hydrogel porogen beads using reactive printing, which we use as templates for creating networks of pores with monomodally distributed pore sizes.

One of the challenges of artificial tissue scaffold engineering is the generation of matrices with controlled, macroporous, open-pored geometry. Soft tissue engineering presents unique challenges: the very high cell density in most soft tissues, often combined with large implant dimensions, means that the supply of oxygen is a critical factor in the success or failure of a soft tissue scaffold.[1] It is known that the pore size has a strong effect on the incorporation of cells into artificial tissues, and the ability to control the scaffold pore size is important for regulating cell responses, such as neovascularization.[2] Without an open, porous geometry to allow the diffusion of oxygen and nutrients into a scaffold, as well as carbon dioxide and other metabolites out, it is difficult to prepare functional scaffolds thicker than several hundred microns.[3] With this as the motivation, we set out to develop a means of preparing open-pored polymeric structures.

Numerous approaches have been taken to develop macroporous materials over the years, including laser ablation, building hydrogels layer-by-layer, and using supercritical carbon dioxide as a porogen.[4] Other approaches involve the addition of inorganic salts as porogens that are less soluble at one pH, and are freely soluble at a different pH,[5] or the addition of oil as an emulsion, and then removing the oil afterwards.[6] Several independent groups have recently reported the successful application of hydrogel porogens,[7–9] demonstrating how these soft porogen structures yield products with continuous, open-pore geometry, presumably in part due to the fact that when packed, the material deforms slightly, resulting in a more open-pore structure.

While the reported techniques using hydrogel porogens have indeed yielded materials with open geometries, the reported methods share a remaining limitation in common with regards to control over the exact diameter. Ideally, the size of the porogens should be programmable, yielding specific, tuneable pore geometry in the range of tens to hundreds of microns, *i.e.* dimensions matching those of cells and capillaries. Building on this motif,[10,11] we have applied inkjet printing as a rapid tool for reactive processing of hydrogels for preparing porogens. In this communication, we would like to report our new approach to creating macroporous structures with controlled, open-pore geometry involving the use of ion-reversible porogenic microspheres with diameters in the range of 50 to 400 μm.[12] To prepare porogenic structures with well-defined geometries, inkjet technology is used to dispense droplets of sodium alginate solution with nearly monodisperse diameters into a hardening bath of calcium chloride (Fig. 1). Calcium alginate hydrogels are stable at a wide range of pH values and other conditions,[13,14] and are readily soluble in the presence of strong calcium-coordinating ligands, such as sodium EDTA.

To prepare the macroporous matrices, the aforementioned spheres are removed from the hardening bath, washed, and then re-suspended in a second solution of a different crosslinkable solution (Fig. 2). As the surrounding solution is crosslinked, the net result is a microcomposite of a crosslinked hydrogel, with embedded porogen microspheres. During the second step, the microcomposite is treated with a trisodium EDTA solution, reversing the alginate crosslinking step, liquefying the beads. The solubilized bead material is washed out, yielding a hydrogel network with an open, macroporous structure.

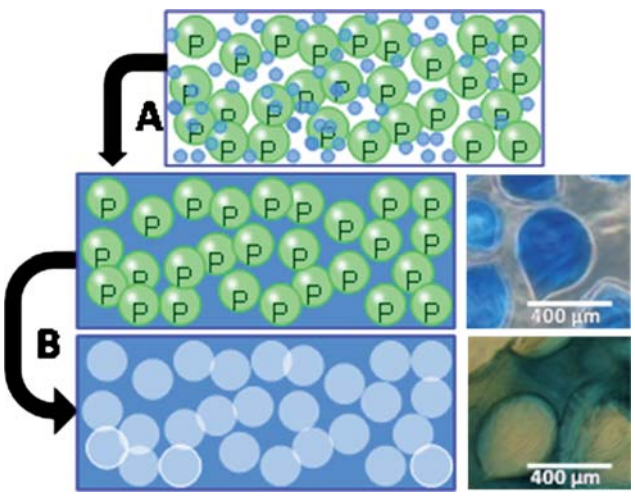

Fig. 1 Process of preparing macroporous hydrogels using porogen microspheres, where: (A) the surrounding alginate is crosslinked and (B) the alginate hydrogel is solubilized.

[a]*Eindhoven University of Technology, Laboratory of Macromolecular Chemistry and Nanoscience, P.O. Box 513, NL-5600 MB Eindhoven, The Netherlands*
[b]*Laboratory of Organic and Macromolecular Chemistry, Friedrich-Schiller-Universität Jena, Humboldtstr. 10, D-07743 Jena, Germany. E-mail: ulrich.schubert@uni-jena.de; Fax: +49(0) 3641 9482 02; Tel: +49(0) 3641 948200*
[c]*Dutch Polymer Institute (DPI), P.O. Box 902, 5600 AX Eindhoven, The Netherlands*

† Electronic supplementary information (ESI) available: Characterization of alginates and printer setup. See DOI: 10.1039/b922888h

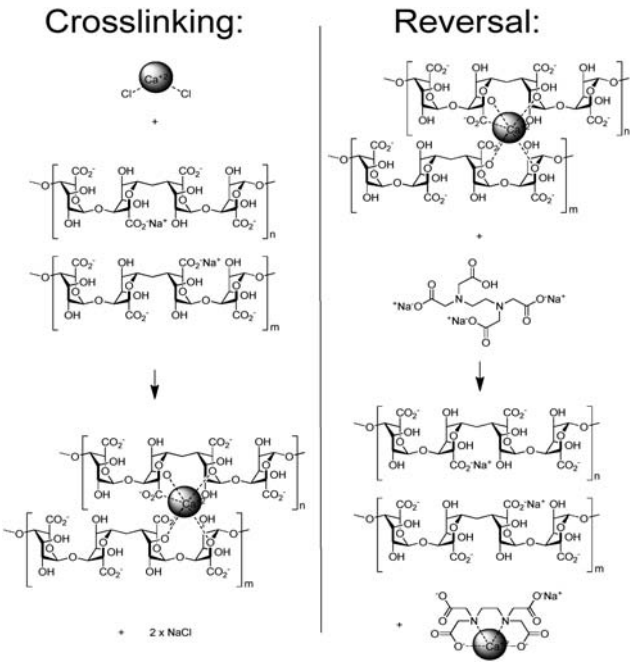

Fig. 2 Reversible crosslinking of alginate by dications: during the crosslinking, calcium forms highly stable complexes with alginate to form networks, while during the reversal, a competing ligand such as EDTA chelates with calcium, and the crosslinking is reversed.

This approach allows for direct control of the macropore size on a scale relevant to cell culturing and tissue engineering. Moreover, this approach may be readily scaled up to make macroporous structures of arbitrarily large sizes (multi-millimetre to multi-centimetre), such as those needed for artificial tissues and organs, while maintaining control of the pore geometry on a multi-micron scale.

By packing the material with a sufficiently high concentration of hydrogel beads in the macroporous matrix, the beads will come into contact with one another, yielding a continuous 3D network of channels once they are removed. While an ideal, face-centered ordered hexagonal packing of spheres will yield a volumetric density of roughly 0.74048 (*i.e.* when the spheres are ideally packed together in a closed container, approximately 74.048% of the total volume is occupied by spheres, and the remaining volume corresponds to interstitial spaces between them),[15,16] a much more realistic expectation is that the spheres will pack randomly, either random loose-packing or random close-packing, depending on the conditions,[17] with random loose-packing values around 0.55,[18–20] and random close-packing in the region of 0.64.[20–22]

In our work, we have examined the use of two separate inkjet printing technologies, including both a drop-on-demand-based technology as well as a continuous ink system. Namely, we made use of the Autodrop piezo-driven drop-on-demand printing system, and the MJ-E-130 Dropjet continuous printing system—both manufactured by Microdrop Technologies GmbH (Norderstedt, Germany). While both are inkjet technologies and can deliver highly reproducible, sub-nanolitre droplets, the two techniques differ considerably in terms of their throughput and the sizes of the droplets generated. In both cases, a 1 wt% sodium alginate solution was prepared in distilled water, and was loaded with an additional 0.01 wt% of brilliant blue G to provide contrast; this solution was filtered, and used as is.

In the case of the drop-on-demand printing, the resulting beads exhibited a highly uniform teardrop shape (Fig. 3a), with an average size of 48 ± 4 μm, and a monomodal size distribution. The beads prepared using the Dropjet continuous inkjet system resulted in considerably larger beads, with an average diameter of 248 μm ± 42 μm; while the size distribution was larger, the distribution was still monomodal (Fig. 3b). These size distributions for alginate porogens are much narrower than those reported for alginate porogen beads prepared under emulsion conditions (450–630 μm to 630–900 μm),[9] as well as reported gelatin beads prepared by oil immersion (100–500 μm),[8] and manual dropcasting and drying alginate (1 800 μm when hydrated).[7] Moreover, the use of drop-on-demand inkjet printing afforded soft, spherical porogens with narrowly defined size distributions in a size range that is otherwise inaccessible by other techniques.

When comparing the two techniques, each offers very different performance characteristics. The droplets afforded by drop-on-demand inkjet printing are much smaller and more uniform in terms of size (Fig. 3). Depending on the application, this considerable size difference between the two may make one technique more advantageous over the other; if the goal is to mimic structures on a single cell level, the drop-on-demand comes closer; however, for preparing larger structures (such as cavity roughly the size of a cavity of a small blood vessel, excluding the endothelial layer), then the continuous inkjet technique has the advantage. The biggest difference in performance, however, is with regards to material throughput: where continuous inkjet printing is roughly three orders of magnitude faster for a single nozzle (*i.e.* 0.5 mL h^{-1} for drop-on-demand, *vs.* 600 mL h^{-1} for continuous inkjet.) While both methods are technically feasible, the ability to produce a thousand-fold larger amount of beads with continuous inkjet printing made this approach more attractive for subsequent testing.

To prepare the macroporous matrix, the slurry of beads was allowed to settle to the bottom of a culture flask, and the natant liquid was decanted off, and replaced with distilled water. The mixture was shaken, and allowed to settle, and the natant liquid was removed again; this process was repeated three times to wash the beads prior to further processing, and then the remaining natant liquid was poured

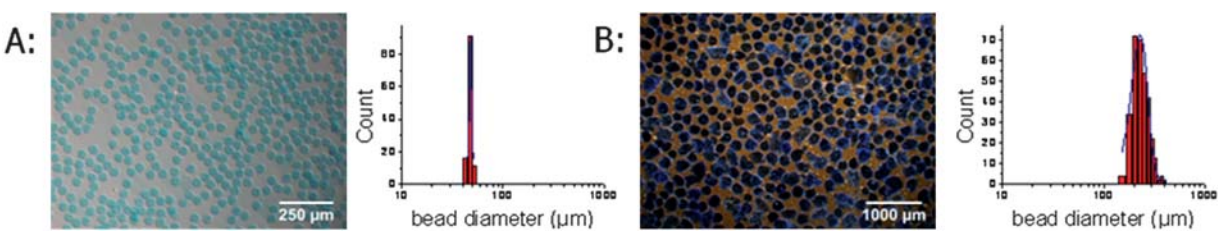

Fig. 3 Microscopy images of beads, and size distribution of beads (A: drop-on-demand, and B: continuous inkjet).

off. The surrounding matrix was prepared using polyethylene glycol dimethacrylate (PEG-DMA; MW = 750 g mol^{-1}), using a redox-initiated polymerization reaction. To accomplish this, a pre-gel solution was prepared from an aliquot of 1 mL of PEG-DMA and 1 mL of *N*,*N*,*N*′,*N*′-tetramethylethylenediamine dissolved in 9 mL of distilled water. A 1 mL aliquot of the pre-gel solution was combined with an equal volume of alginate beads in a 4 mL GC vial, mixed, and allowed to settle. After settling, the natant solution was removed, and a drop of 20 wt% ammonium persulfate was deposited on the top of the mixture; within seconds, the polymerization reaction was evident, as the surrounding solution where the droplet was deposited was transformed from clear to an opaque gel, and the reaction continued to propagate through the mixture until it reached the bottom of the vial. After about 5 min, the reaction was complete. The vial was cracked open to remove the crosslinked sample.

In order to get a more statistical understanding of the size and size distribution of the beads, low resolution inverted light microscopy coupled with software-assisted image analysis was chosen as the analytical method for this task. The steps taken in digital processing were found to be critical for reliably measuring images of large numbers of particles: in order for objects to be automatically measured by the software ImageJ, the image must be converted into a binary set of highlighted, distinct objects on a non-interfering background, which requires the judicious use of filters, color corrections, and other image processing tools to make them readable. Developing the right combination of settings was critical to making these structures measurable. An example of the process used can be seen in Fig. 4.

Briefly, a fast-Fourier transform bandpass filter was used to even out shadows in the image, followed by automated color optimization; next, the RGB color channels were split, and the red channel was separated and then converted to a binary image. The threshold of the binary was adjusted so that the structures to be measured were highlighted, and then watershed segmentation was used to separate particles that were touching. Once these steps were accomplished, the processed image could be measured using the analyze particles feature in the software, which generates a table outlining the measurements for the particles in the image; once this is obtained, the data can then be analyzed and graphed using software such as OriginPro 8G. Following these steps, hundreds of particles can easily be measured in an automated, uniform, and reliable way.

The crosslinked material was subsequently sliced into 15 μm sections using a microtome, and then treated with a 10 wt% EDTA solution to remove the alginate. During this process, it was observed that upon treatment with EDTA, the brilliant blue G dye transferred from the alginate material into the PEG-DMA matrix material, staining the PEG-DMA structures blue. The resulting material was examined using an inverted light microscope (Fig. 5). In this image, the blue areas correspond to the crosslinked macroporous matrix, and the light areas are the pores remaining after the dissolution of alginate by treatment with EDTA. Based on the percentage of area covered by the remaining crosslinked matrix, the porosity of the material was estimated to be 0.45, which would correspond to what one would expect for random loose packing of the hydrogel spheres.

In conclusion, using both drop-on-demand and continuous inkjet printing techniques, we prepared calcium alginate beads with well-defined geometries. By taking advantage of their reversible gel state, they were effectively employed as hydrogel porogen materials, offering access to macroporous matrix materials with open pore

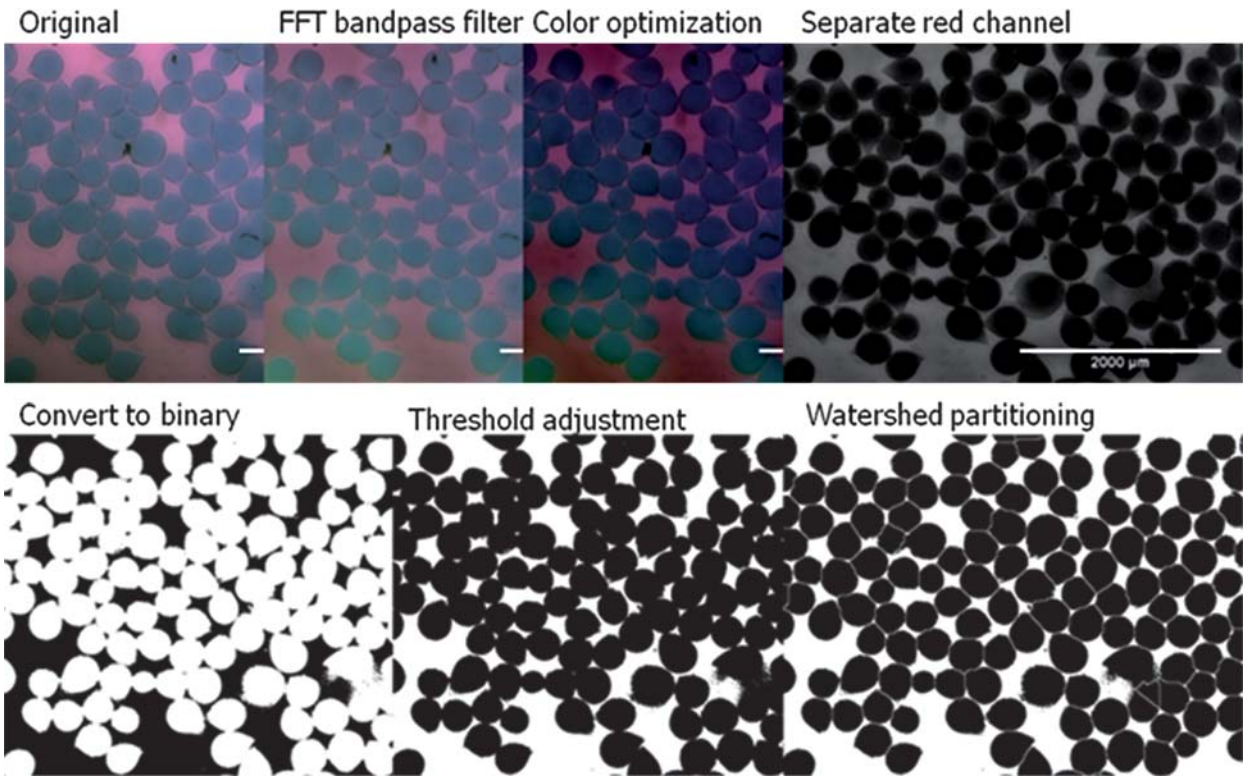

Fig. 4 Typical image processing steps involved in the analysis of the alginate particles using the ImageJ image analysis software.[23]

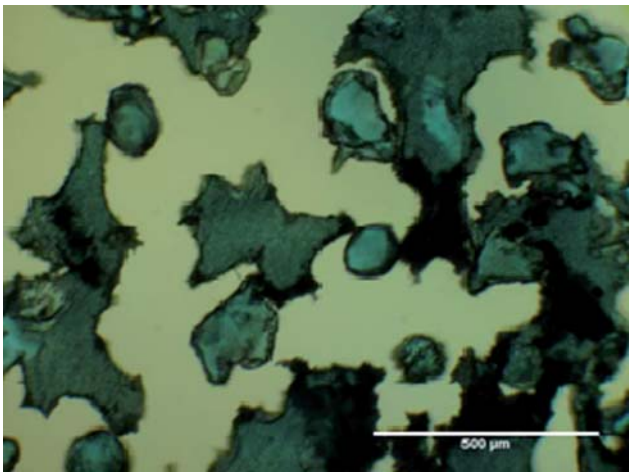

Fig. 5 Microtomy image of the hydrogel structure.

geometries. The alginate beads and the resulting matrix materials were characterized using optical microscopy coupled with image analysis tools to make the process more automated.

Inkjet printing allows for dispensing liquids in aliquots that match roughly the dimensions of animal cells and small tissue structures. This new interplay afforded by inkjet printing between reversible hydrogels and micron-scale processing results in a wide range of possibilities for new programmable materials and devices, with unique structural features. While the original motivation for this work was driven by interest in macroporous matrices for tissue engineering, the ability to control pore size has broader applications. This facile strategy to materials with 3D macro-scale size control should be useful for creating a whole host of new and interesting materials.

Notes and references

1 T. I. Croll, S. Gentz, K. Mueller, M. Davidson, A. J. O'Connor, G. W. Stevens and J. J. Cooper-White, *Chem. Eng. Sci.*, 2005, **60**, 4924.
2 D. Druecke, S. Langer, E. Lamme, J. Pieper, M. Ugarkovic, H. U. Steinau and H. H. Homann, *J. Biomed. Mater. Res.*, 2004, **68a**, 10.
3 K. Kellner, G. Liebsch, I. Klimant, O. S. Wolfbeis, T. Blunk, M. B. Schulz and A. Gopferich, *Biotechnol. Bioeng.*, 2002, **80**, 73.
4 A. I. Cooper and A. B. Holmes, *Adv. Mater.*, 1999, **11**, 1270.
5 M. V. Badiger, M. E. McNeill and N. B. Graham, *Biomaterials*, 1993, **14**, 1059.
6 H. Tokuyama and A. Kanehara, *Langmuir*, 2007, **23**, 11246.
7 S. Hamasaki, A. Tachibana, D. Tada, K. Yamauchi and T. Tanabe, *Mater. Sci. Eng., C*, 2008, **28**, 1250.
8 J. Kim, M. J. Yaszemski and L. Lu, *Tissue Eng., Part C*, 2009.
9 G. H. Yu and Y. B. Fan, *J. Biomater. Sci., Polym. Ed.*, 2008, **19**, 87.
10 B. J. de Gans, P. C. Duineveld and U. S. Schubert, *Adv. Mater.*, 2004, **16**, 203.
11 E. Tekin, P. J. Smith and U. S. Schubert, *Soft Matter*, 2008, **4**, 703.
12 J. T. Delaney, U. S. Schubert, PCT Eur. Appl. Patent EP08018399.9, 2008.
13 D. L. Cohen, E. Malone, H. Lipson and L. J. Bonassar, *Tissue Eng.*, 2006, **12**, 1325.
14 O. Smidsrod, *Faraday Discuss. Chem. Soc.*, 1974, **57**, 263.
15 C. A. Rogers, *Proc. London Math. Soc.*, 1958, **s3–8**, 609.
16 T. C. Hales and S. P. Ferguson, *Discrete Comput. Geom.*, 2006, **36**, 21.
17 C. Song, P. Wang and H. A. Makse, *Nature*, 2008, **453**, 629.
18 G. D. Scott and D. M. Kilgour, *J. Phys. D: Appl. Phys.*, 1969, **2**, 863.
19 G. Y. Onoda and E. G. Liniger, *Phys. Rev. Lett.*, 1990, **64**, 2727.
20 J. G. Berryman, *Phys. Rev. A: At., Mol., Opt. Phys.*, 1983, **27**, 1053.
21 J. D. Bernal and J. Mason, *Nature*, 1960, **188**, 910.
22 G. D. Scott, K. R. Knight, J. D. Bernal and J. Mason, *Nature*, 1962, **194**, 956.
23 W. Rasband, freely available at: http://rsb.info.nih.gov/ij/.